Mihajlo Aranđelović[1], Simon Sedmak[1], Ana Petrović[2], Stefan Dikić[3], Radomir Jovičić[1], Branislav Đorđević[1], Aleksandar Sedmak[2], Vojin Milić[4], Miroslav Duspara[5]*

ANALYSIS OF FERRITIC-AUSTENITIC WELDED JOINT BEHAVIOUR UNDER TENSION BY USING FINITE ELEMENT METHOD AND DIGITAL IMAGE CORRELATION

ANALIZA PONAŠANJA FERITNO-AUSTENITNOG ZAVARENOG SPOJA PRI ZATEZANJU PRIMENOM METODE KONAČNIH ELEMENATA I DIGITALNOM KORELACIJOM SLIKA

Originalni naučni rad / Original scientific paper
Rad primljen / Paper received: 10.04.2026
https://doi.org/10.69644/ivk-2026-02-0217
Adresa autora / Author's address:
[1] Innovation Centre of the Faculty of Mechanical Engineering, Belgrade, Serbia M. Aranđelović https://orcid.org/0000-0002-5040-5167 ; S. Sedmak https://orcid.org/0000-0002-2674-541X ; B. Đorđević https://orcid.org/0000-0001-8595-6930
[2] University of Belgrade, Faculty of Mechanical Engineering, Belgrade, Serbia A. Petrović https://orcid.org/0000-0002-5996-1485 ; A. Sedmak https://orcid.org/0000-0002-5438-1895
[3] University of Belgrade, Faculty of Technology and Metallurgy, Belgrade, Serbia S. Dikić https://orcid.org/0000-0003-2700-0628
[4] TUV Rheinland InterCert d.o.o., Belgrade, Serbia
[5] University of Slavonski Brod, Faculty of Mechanical Engineering, Slavonski Brod, Croatia M. Duspara https://orcid.org/0000-0003-4249-9279 , *email: simon.sedmak@structuralintegrity.eu

Keywords
- ferritic-austenitic welded joint
- tensile properties
- finite element method
- digital image correlation

Abstract

Research presented here deals with the behaviour of heterogeneous welded joints, made of steels with very different mechanical properties, especially in terms of plasticity. This stage of the research includes experimental tensile tests with digital image correlation as a means of monitoring the deformation of specimens, and numerical simulations that are based on these results, where good agreement is shown. Due to the notable importance of heterogeneous welded joints in practical applications, this analysis continues to further develop, focusing on welded joints with defects.

Ključne reči
- feritno-austenitni zavareni spojevi
- zatezne osobine
- metoda konačnih elemenata
- digitalna korelacija slika

Izvod

Prikazano istraživanje se bavi ponašanjem heterogenih zavarenih spojeva, napravljenih od čelika, veoma različitih mehaničkih svojstava, posebno u pogledu plastičnosti. Ova faza istraživanja obuhvataju eksperimentalna zatezna ispitivanja, sa digitalnom korelacijom slika kao sredstvom praćenja deformacija uzoraka, i numeričke simulacije koje su zasnovane na ovim rezultatima, a koje pokazuju dobro međusobno slaganje. Zbog značaja heterogenih zavarenih spojeva u praktičnoj primeni, ova analiza se dalje razvija, sa fokusom na zavarene spojeve sa greškama.

INTRODUCTION

Ferritic-austenitic (F-A) steel welded joints are commonly encountered in practice, especially in oil and energy industry. In these cases, various elements and equipment are made of such materials, typically using ferritic steel for supports and pipelines, whereas austenitic steel like the S304 and S316 series, are used for structures subjected to corrosive environments, including also load-bearing elements and pressure vessels. There are numerous examples of the application of dissimilar joints, /1/, investigating welded joints in petroleum distillation towers with focus on optimal heat input during welding to ensure proper corrosion resistance of these joints. In /2/, more general analysis of dissimilar welds is provided, as well as the use of different welding processes to determine the optimal one. As in this paper, steel S304 is also used as one of the austenitic components of the welded joint.

Dissimilar ferritic-austenitic steels are also encountered in the nuclear industry. Paper /3/ provides an overview of numerous failures of such joints and describes an extensive experimental analysis on how to improve their integrity. It also mentions the influence of specific welding defects on the microstructure, and the issues that may result from their presence. Failure in dissimilar welds can also occur within the HAZ or the fusion line, which is of particular interest in the research presented here, as described in /3, 4/.

Welding of F-A steels typically involves issues related to heat input and defects, due to significant differences between their properties. Even more important than significant difference in chemical compositions of a low-alloyed low-carbon steel (S355) and high-alloyed stainless steel (S304) are the different coefficients of thermal expansion /5/. Due to this, the deformation during welding will differ considerably between the austenitic and ferritic side, and this needs to be taken into account to avoid high residual stresses. It also results in different requirements for heat input, which must be controlled more strictly in the case of austenitic steels. Thus, welding defects that will occur in the joint could be very different from what would be expected if the same material is used on both sides of the weld. Furthermore, when determining the properties of the heat affected zone by numerical iterative method /6, 7/, it should be taken into account that there are two distinctive heat affected zones in these welded joints - the one between the ferritic material and weld metal, and the one between the weld metal and austenitic material, with their own respective mechanical properties.

Another important issue with F-A welded joints is the significant difference in strain at failure, which is much higher for the S304 steel. However, its yield stress is lower compared to S355, which affects the way in which welded joint specimens deform in the experiment, and consequently, the numerical simulation, which will be shown in more detail in the following chapters.

Welded joints are produced on plates of high alloyed austenitic steel (SS304L) and common structural ferritic steel (S355J2). Their typical application is for low temperature pressure vessels, as in the case of CO_2 storage tanks, made by welding of rolled and bended plates. At the same time, since attachments as small pipes are not produced of these steels, another type of steel has to be used, like high alloyed austenitic steel, also suitable for low temperature applications. Welding of such a combination of steels is not a simple task, not only due to the heterogeneity of materials and mechanical properties, but also due to different physical properties, mostly related to heat. From both points of view F-A welded joints are prone to defects, including micro-cracks. Furthermore, if heterogeneous joints are to be made of these two types of steel, one has to take into account that austenitic steel has a 100 °C lower melting temperature, 20 % higher specific heat, 3 times lower heat conductivity, 5 times higher electrical resistance and a 50 % higher thermal linear coefficient. More detailed description of all aforementioned problems is given in /1/.

MATERIALS AND WELDING

Two base metals (BM), S355J2 and SS304L are used to produce the welded joint by Gas Shielded Arc Welding (GSAW) with austenitic welding wire. Tensile properties of the welding wire are: YS ≥ 380 MPa, UTS = 560-660 MPa, $A_5 \geq 35\%$. Chemical composition is shown in Table 1 for both BMs.

Table 1. Chemical composition of two BMs and welding wire.

	C	S	P	Mn	Si	Cr	Mo	Ni	Cu	V	Co
SS304L	0.03	0.0005	0.0378	1.8	0.36	18.1	04	8.2			0.01
S355J2	0.13	0.0009	0.0087	1.0	0.21	0.18	0.04	0.18	0.35	0.08	0.15
Welding wire	0.08			7.0	≤1.0	18.5		9.0			

STRESS-STRAIN CURVES

Stress-strain curves are obtained using universal tensile machine. Results for both BMs (ferrite and austenite), the welded joint (WJ) as a whole, and WM, are shown in Figs. 1-4, respectively. As one can see, WJ as a whole behaves similarly to the ferrite BM, with somewhat larger elongation A_5, whereas WM behaves similarly to the austenite BM, with somewhat smaller A_5.

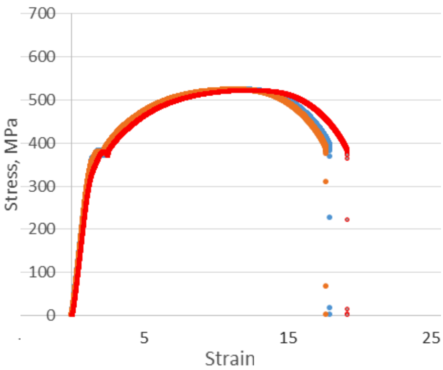

Figure 1. Stress-strain curve - ferrite BM: YS = 375 MPa, UTS = 523 MPa, A_5 = 18.1 % (S355J2).

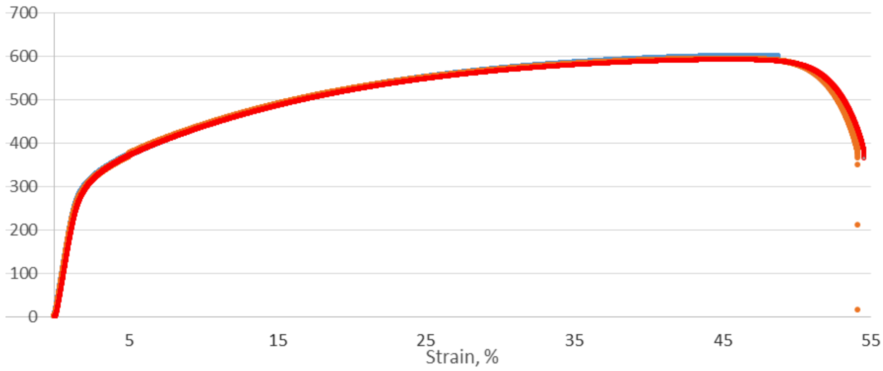

Figure 2. Stress-strain curve - austenite BM: YS = 305 MPa, UTS = 595 MPa; A_5 = 61.4 % (SS304L).

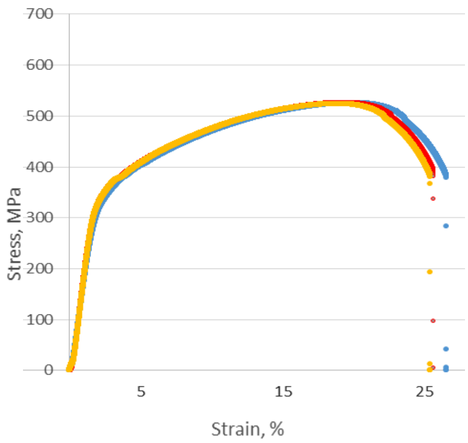

Figure 3. Stress-strain curve - WJ as a whole: YS = 360 MPa; UTS = 525 MPa; A_5 = 26.5 %.

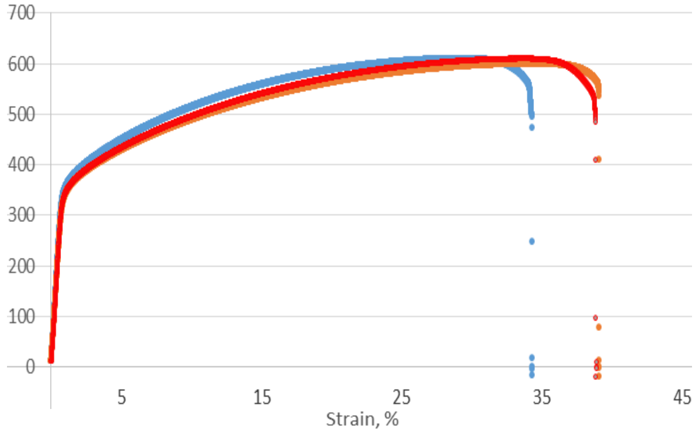

Figure 4. Stress-strain curve - WM: YS = 360 MPa; UTS = 600 MPa; A_5 = 38 %.

RESULTS

Digital image correlation

Digital Image Correlation (DIC) is used to measure strains during tensile tests, including plastic deformation after reaching yield stress, /8-11/. As a result of experimental testing the whole strain field is obtained in all stages of loading, including all zones of the welded joint, however small they might be. This feature of DIC enables application of a relatively simple iterative procedure to assess tensile properties of HAZ which is otherwise difficult, if not impossible to obtain, /12/. Toward this aim, in initial FEM models, material properties of HAZ are assumed and then the results compared with experimental ones obtained by DIC. Based on the difference between them, corrections of HAZ tensile properties are applied in the following iterations until the difference becomes small enough, as explained in more detail in /12/. Results of DIC measurements are shown in Fig. 5 for a couple of load levels, represented in stages (70, 110, 140 and 170), where stage 170 corresponds to 450 MPa remote stress providing 18 % of plastic strain.

a)
b)
c)

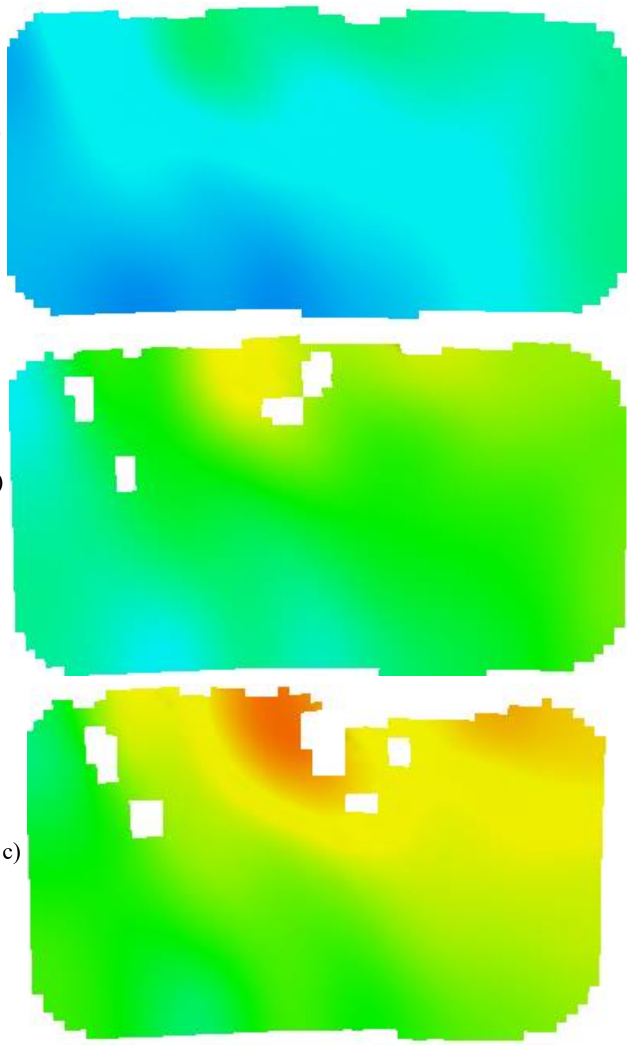

d)

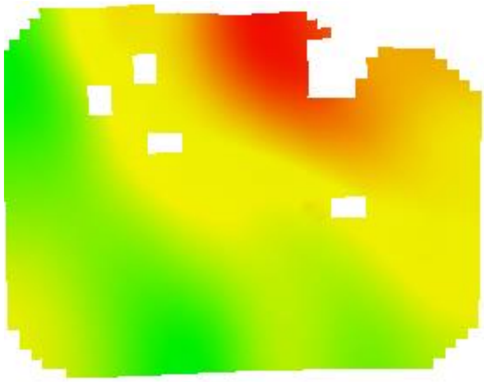

Figure 5. DIC stages: a) 70; b) 110; c) 140; d) 170 (maximal strain 18 %).

FE ANALYSIS AND DISCUSSION

Finite element analysis is performed in ABAQUS®, commonly used for this type of analyses, as in /6, 7, 13-17/. The finite element mesh is generated using linear HEX elements, size 4.5 mm, with refinement in critical areas where element size is 0.5-1 mm, Fig. 6.

Boundary conditions are shown in Fig. 7, where one side (ferrite) is fixed, the loading is defined on the opposite side, total force 150 kN, as in the experiment, resulting in remote stress of 500 MPa.

Tensile properties are defined in form of YS and H' calculated in ANSYS as the difference between YS and maximal stress is divided by corresponding strain. As already mentioned, YS and H' are obtained either directly from the stress-strain curves (austenite BM, ferrite BM and WM) or by iteration procedure (both HAZs), as shown in Table 2.

Table 2. Tensile properties used for numerical analyses.

	HAZ austenite BM	HAZ ferrite BM	Austenite BM	Ferrite BM	WM
YS (MPa)	360	425	295	375	355
H' (MPa)	3667	4050	1540	1610	1720

To verify the FE analysis, the equivalent strain distribution at 440 MPa remote stress is compared with the corresponding DIC measurement, Fig. 8. As one can see, the maximal strain is 0.7 % (HAZ of austenite BM), both by FE analysis and DIC measurement.

Results of FE analysis are shown in the form of equivalent plastic strain PEEQ, (Fig. 9), maximal strain E, (Fig. 10) and von Mises stress S in the two presentation modes, Fig. 11. As one can see, the maximum von Mises stress, 741 MPa, is located in the HAZ of ferrite BM (due to stress concentration), whereas the maximal strain is in austenite BM (since its yield stress is the lowest), although the specimens broke in the ferrite BM since the stress reached its UTS first (the lowest one, 525 MPa). Hence, it can be seen that good agreement between the numerical and experimental results is achieved.

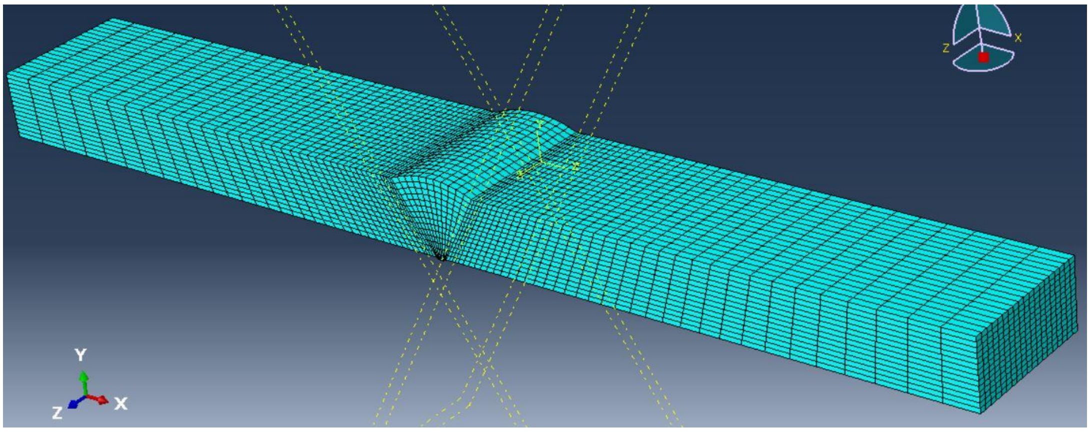

Figure 6. FE mesh.

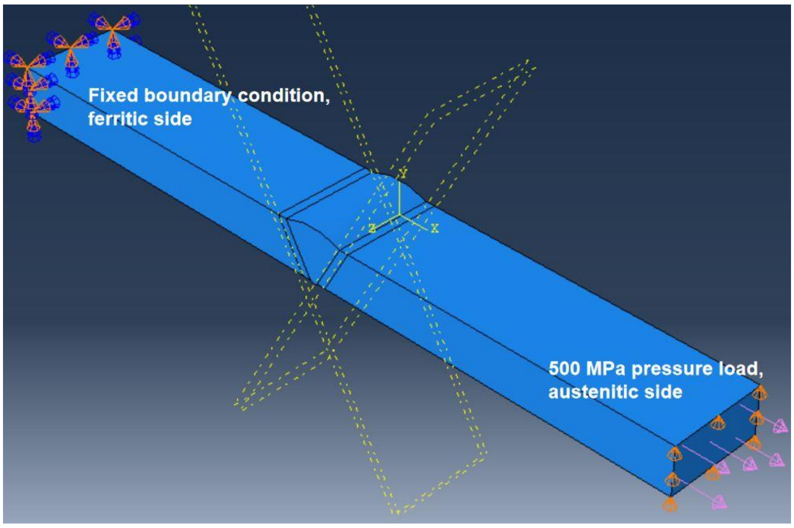

Figure 7. Boundary conditions.

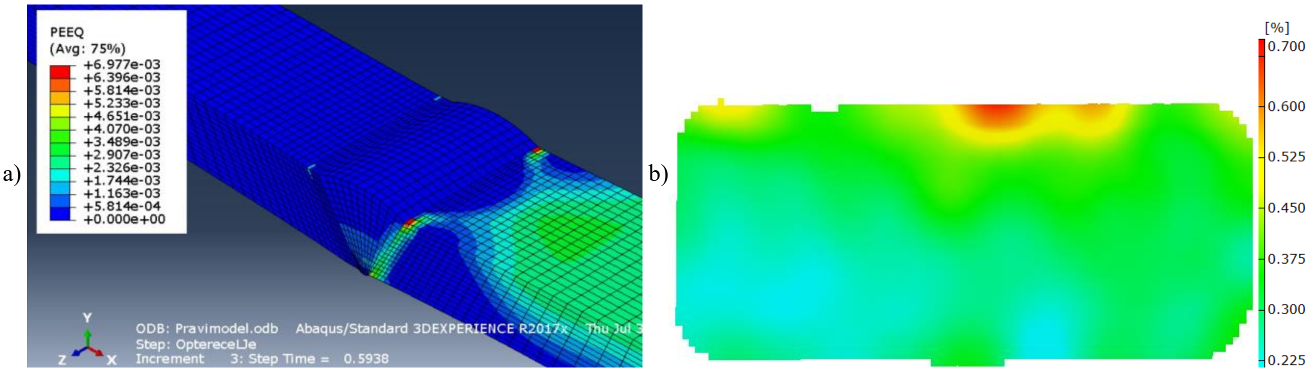

Figure 8. a) FEM equivalent strain distribution compared to b) DIC at remote stress 440 MPa.

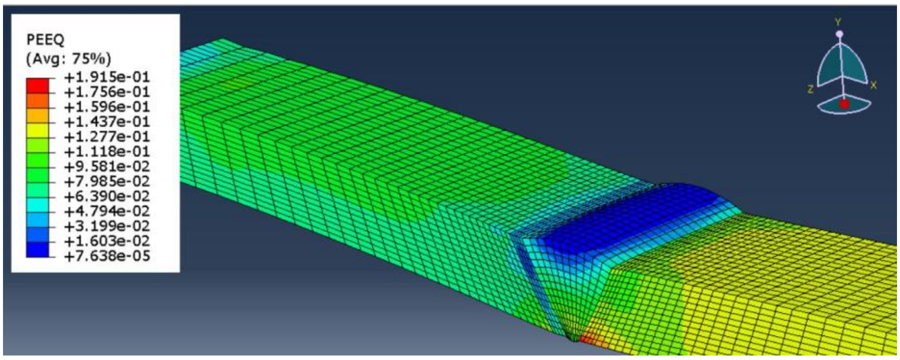

Figure 9. Equivalent strain, max. 19 % in BM A, cca. 12 % in BM F at failure location (in accordance with tensile curve, Fig. 1), force 150 kN, remote stress 500 MPa.

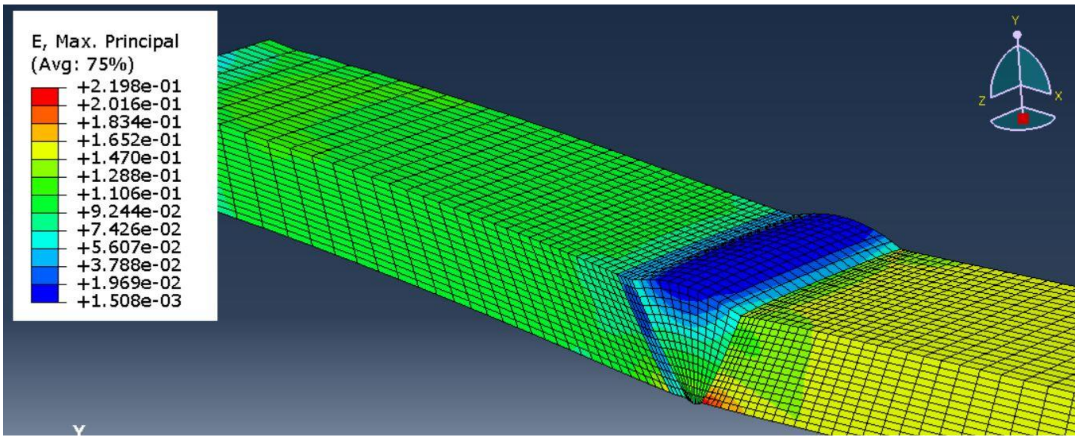

Figure 10. Maximal strain 22 % in BM A, cca. 14 % in BM F at failure location (in accordance with tensile curve, Fig. 1), force 150 kN, remote stress 500 MPa.

a)
b)

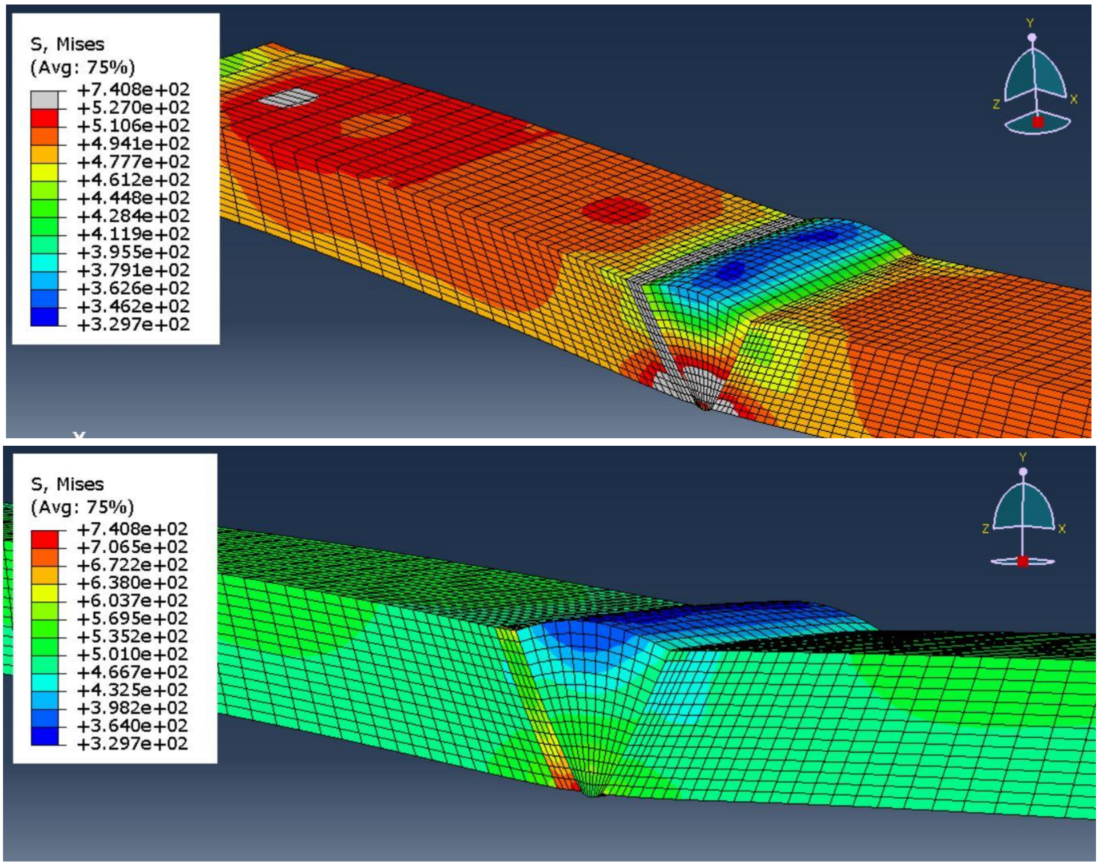

Figure 11. Von Mises stress distribution: a) maximal stress areas in grey; b) maximal stress 741 MPa in HAZ of ferrite BM.

CONCLUSIONS

Based on the experimental and numerical analysis of the F-A welded joint under tension presented in this paper, the following can be concluded:

- BM A starts to yield first since it has the lowest yield stress, followed by BM F and WM. The BM F breaks first since it has the lowest UTS.
- Tensile properties of HAZ are successfully determined by using iterative FE calculations and their comparison with DIC results.
- Further analysis of F-A welded joints with defects should follow, based on the results presented here, using experimental and numerical analysis in the same way.

ACKNOWLEDGEMENTS

Authors would like to express their gratitude to the Ministry of Education, Science and Technological Development, Republic of Serbia, Grant no. 451-03-47/2023-01/200213, for supporting our work.

REFERENCES

1. Silva, C.C., Miranda, H.C., de Sant'Ana, H.B., Farias, J.P. (2013), *Austenitic and ferritic stainless steel dissimilar weld metal evaluation for the applications as-coating in the petroleum processing equipment*. Mater. Des. 47: 1-8. doi: 10.1016/j.matdes.2012.11.048

2. Ambade, S., Khan, F., Dahikar, A., et al. (2024), *Dissimilar welding of austenitic SS and ferritic SS in last decades*, Mater. Today: Proc. 100: 45-50. doi: 10.1016/j.matpr.2023.04.533
3. Rathod, D.W., Pandey, S., Singh, P.K., Prasad, R. (2015). *Experimental analysis of dissimilar metal weld joint: Ferritic to austenitic stainless steel*, Mater. Sci. Eng.: A, 639: 259-268. doi: 10.1016/j.msea.2015.05.011
4. DuPont, J.N. (2012), *Microstructural evolution and high temperature failure of ferritic to austenitic dissimilar welds*, Int. Mater. Rev. 57(4): 208-234. doi: 10.1179/1743280412Y.0000000006
5. Joseph, A., Rai, S.K., Jayakumar, T., Murugan, N. (2005), *Evaluation of residual stresses in dissimilar weld joints*, Int. J Press. Ves. Piping, 82(9): 700-705. doi: 10.1016/j.ijpvp.2005.03.006
6. Aranđelović, M., Petrović, A., Đorđević, B., et al. (2023), *Effects of multiple defects on welded joint behaviour under the uniaxial tensile loading: FEM and experimental approach*, Sustainability, 15(1): 761. doi: 10.3390/su15010761
7. Arandjelovic, M., Djordjevic, B., Sedmak, S., et al. (2024), *Failure analysis of welded joint with multiple defects by extended Finite Element Method and Engineering Critical Analysis*, Eng. Fail. Anal. 160: 108176. doi: 10.1016/j.engfailanal.2024.108176
8. Peters, W.H., Ranson, W.F. (1982), *Digital imaging techniques in experimental stress analysis*, Optic. Eng. 21(3): 213427. doi: 10.1117/12.7972925
9. Sutton, M.A., Wolters, W.J., Peters, W.H., et al. (1983), *Determination of displacements using an improved digital correlation method*, Image Vision Comput. 1(3): 133-139. doi: 10.1016/0262-8856(83)90064-1
10. Chu, T.C., Ranson, W.F., Sutton, M.A. (1985), *Applications of digital-image-correlation techniques to experimental mechanics*, Exper. Mech. 25(3): 232-244. doi: 10.1007/BF02325092
11. Aranđelović, M., Petrović, A., Sedmak, S. (2024), *Digital image correlation application to structural integrity assessment*, Struct. Integr. Life, 24(1): 87-91. doi: 10.69644/ivk-2024-01-0087
12. Petrović, A., Momčilović, N., Đorđević, B., et al. (2025), *Inverse iterative methodology for welded joints characterization in construction designing and comparison to classical approach*, Acta Polytechnica Hungarica, 22(4): 45-63. doi: 10.12700/APH.22.4.2025.4.4
13. Solob, A., Grbović, A., Božić, Ž., Sedmak, S. (2020), *XFEM based analysis of fatigue crack growth in damaged wing-fuselage attachment lug*, Eng. Fail. Anal. 112: 104516. doi: 10.1016/j.engfailanal.2020.104516
14. Nikfam, M.R., Zeinoddini, M., Aghebati, F., Arghaei, A.A. (2019), *Experimental and XFEM modelling of high cycle fatigue crack growth in steel welded T-joints*, Int. J Mech. Sci. 153-154: 178-193. doi: 10.1016/j.ijmecsci.2019.01.040
15. Xu, J., Sun, K., Quiang, X., et al. (2023), *XFEM-based fatigue crack propagation analysis on key welded connections of orthotropic steel bridge deck*, Int. J Steel Struct. 23(2): 404-416. doi: 10.1007/s13296-022-00701-3
16. Grbović, A., Kastratović, G., Sedmak, A., et al. (2019), *Fatigue crack paths in light aircraft wing spars*, Int. J Fatigue, 123: 96-104. doi: 10.1016/j.ijfatigue.2019.02.013
17. Đurđević, A., Živojinović, D., Grbović, A., et al. (2015), *Numerical simulation of fatigue crack propagation in friction stir welded joint made of Al 2024-T351 alloy*, Eng. Fail. Anal. 58: 477-484. doi: 10.1016/j.engfailanal.2015.08.028